Chemical Physics Letters 467 (2009) 255–259

Contents lists available at ScienceDirect

Chemical Physics Letters

journal homepage: www.elsevier.com/locate/cplett

# IR–UV double resonance spectra of pyrazine dimers: Competition between CH···π, π···π and CH···N interactions

Matthias Busker, Yuriy N. Svartsov, Thomas Häber, Karl Kleinermanns *

*Institut für Physikalische Chemie, Heinrich-Heine Universität Düsseldorf, Universitätsstr. 1, 40225 Düsseldorf, Germany*

ARTICLE INFO

*Article history:*
Received 11 August 2008
In final form 6 October 2008
Available online 27 November 2008

ABSTRACT

We present size- and isomer-selective IR–UV double resonance spectra of two pyrazine dimer isomers. The most stable isomer has a planar structure, stabilized by two CH···N contacts. The other isomer has a stacked, cross-displaced structure. Our assignment is supported by B3LYP-D calculations. RI-MP2 calculations tend to overestimate the stability of the stacked and T-shaped isomers.



## 1. Introduction

Weakly polar CH groups are non-conventional hydrogen bond donors whereas aromatic π-systems and triple bonds can act as weak hydrogen bond acceptors. Despite their weakness CH···O, N, π interactions are supposed to significantly contribute to the stabilization of supramolecular aggregates, crystal packing, molecular recognition and folding of proteins. CH···O bonds have been thoroughly investigated in the past [1,2]. They involve an electrostatic interaction, operate over distances beyond the van der Waals limit and are directional. However, much less is known about CH···N interactions (see Ref. [3] and reference therein).

Crystallization of aromatic azacycles like pyridine (Pd) and pyrazine (Pz) and their derivatives enabled the analysis of CH···N networks and supramolecular CH··· N synthons in stoichiometrically defined complexes by X-ray methods [4,5,3]. On the other hand, supersonic expansions allow for the formation of small molecular complexes (clusters) under size-controlled conditions which can be compared to the smallest building blocks of the crystal network. The infrared (IR) spectra of these gas phase complexes are especially sensitive to CH···X interactions because of the induced spectral shifts of the CH stretching vibrations. In combination with resonance enhanced 2-photon ionization (R2PI) and time-of-flight mass detection this provides a powerful tool for mass- and isomer-selective detection of the infrared spectra of different clusters.

While the benzene dimer has been studied by several groups, both theoretically and experimentally [6–14], very little is known about the dimers of the analogous azacycles pyridine, pyrazine and pyrimidine. Two-color R2PI spectra of pyrazine and pyrimidine at various ionization energies revealed several different isomers in supersonic jets [15,16]. In the case of pyrazine two isomers have been identified and assigned to a T-shaped and a planar, doubly CH··· N bridged dimer based on calculations employing a Lennard–Jones as well as a hydrogen bonding potential. Recently Mishra and Sathyamurthy published MP2, MP4 and CCSD(T) calculations of several pyrazine dimer isomers [17]. They found the cross-displaced stacked dimer ($C_S$ symmetry) to be the most stable at the MP2 level, while at the MP4 and CCSD(T) levels the T-shaped dimer with the N-atom of the stem pointing to the top becomes the most stable structure.

In this Letter we report size and isomer selected infrared spectra of pyrazine dimers ($Pz_2$) and compare them to vibrational spectra of various possible dimer structures calculated at the RI-MP2 and DFT-D levels of theory, utilizing the TZVP and TZVPP basis sets.

## 2. Experiment

The basic principles of our IR–UV experimental setup were described in detail elsewhere [21–23]. A gas mixture of about 0.2% pyrazine (Acros Organics, >99%) in helium (Air Liquide, 5.0) was expanded through the 300 μm orifice of a pulsed valve (Series 9, General Valve) at a stagnation pressure of 2 bar. The molecules are cooled down to a few Kelvin in the adiabatic expansion where they form clusters.

The skimmed molecular beam (skimmer diameter 2 mm) crosses the UV excitation laser (LAS, frequency doubled, 10 μJ/ pulse) and the ionization laser (FL 2002, Lambda Physics, frequency doubled, 120 μJ/pulse) at right angle inside the ion extraction region of a linear time-of-flight (TOF) mass spectrometer in Wiley–McLaren configuration. The UV excitation and ionization lasers are spatially and temporally overlapped. Resonant two photon ionization (R2PI) spectra are recorded by scanning the frequency of the excitation laser between 30,820 and 30,940 $cm^{-1}$, while the ionization laser is kept at a fixed wavelength of 233 nm ($\approx 42,918$ $cm^{-1}$) or 235.5 nm ($\approx 42,463$ $cm^{-1}$). Since the pyrazine monomer requires an ionization laser energy of more than 44,000 $cm^{-1}$, the strong monomer signal is effectively suppressed by the selected ionization wavelengths [15,16]. In

* Corresponding author. Fax: +49 211 81 12179.
*E-mail address:* kleinermanns@uni-duesseldorf.de (K. Kleinermanns).

0009-2614/$ - see front matter © 2008 Elsevier B.V. All rights reserved.
doi:10.1016/j.cplett.2008.10.091

addition, the two-color scheme minimizes excess energy in the ions and reduces the amount of fragmentation after ionization.

For the IR/UV double resonance experiments a pulsed IR laser beam (burn laser, 0.2 $cm^{-1}$ resolution) is aligned collinear to the UV excitation beam (probe laser) and fired 150 ns before the latter. The IR laser frequency is scanned over the vibrational transitions and removes vibrational ground state population if resonant, while the UV excitation laser is kept at a frequency resonant with a vibronic transition of a single cluster isomer. By monitoring the ion mass signal as a function of IR frequency, cluster mass and isomer-selective infrared spectra, detected as ion dips, can be obtained. IR laser light is generated by a two-stage setup [24], producing infrared radiation between 2800 and 4000 $cm^{-1}$ (10 Hz, 4 mJ/pulse). The rovibrational transitions of the NH stretching vibrations of ammonia were used for frequency calibration.

The RI-MP2 [25,26] and DFT-D [27,28] calculations were performed with the TURBOMOLE V5.10 program package [29]. Calculated harmonic vibrational frequencies were scaled by 0.9694 (B3LYP-D/TZVP) to match the experimental absorption maximum of the pyrazine monomer C–H stretching vibration at 3070 $cm^{-1}$ [30]. Dimerization energies are not BSSE corrected.

## 3. Results and discussion

Fig. 1 shows the two-color R2PI spectra of the pyrazine dimer $(Pz)_2$ in the region of the pyrazine $S_1$ origin at 30,876 $cm^{-1}$ [31]. The spectra were obtained on the pyrazine dimer mass channel and at different ionization energies. At lower ionization energies (bottom trace) we observed bands at −26, −11, −6, +34 and +51 $cm^{-1}$ relative to the monomer origin. With increasing ionization laser frequency (top trace) the bands at −11, +12 and +26 $cm^{-1}$ gain intensity compared to the others (arrows in Fig. 1), indicating the presence of at least two different isomers. We did not observe any considerable fragmentation of the cluster ions. Below an ionization frequency of 42,000 $cm^{-1}$ no dimer ion signals were observed. The ionization energies used to obtain the spectra in Fig. 1 are still below the ionization threshold of the monomer which is above 44,000 $cm^{-1}$. Overall the R2PI spectra are in agreement with earlier measurements [15]. From now on we will call the isomer with the lower ionization threshold 'isomer 1' and that with the higher ionization threshold 'isomer 2'.

It should be noted that the dimer spectra could be obtained only when the UV excitation and ionization laser pulses (≈10 ns pulse width) were perfectly overlapped in time. No ion signals were observed when delaying the ionization laser by as little as 10 ns with respect to the excitation laser pulse. Thus the excited state lifetime seems to be much shorter than for the monomer, either due to more efficient non-radiative decay channels or due to fragmentation within the electronically excited state.

Fig. 2 shows the IR–UV double resonance spectra of isomers 1 and 2 (top two traces) between 3000 and 3125 $cm^{-1}$ with the UV excitation laser tuned to the respective $0_0^0$ origins at 30,848 $cm^{-1}$ (−27) and 30,863 $cm^{-1}$ (−12). Both isomers were ionized at 233 nm. Also shown is the IR–UV spectrum of the pyrazine monomer (bottom) obtained at its $S_1$ origin (30,876 $cm^{-1}$ [31]) and an ionization wavelength of 193 nm. The monomer shows a single absorption at 3070 $cm^{-1}$ in agreement with the literature [30,32].

Interestingly, the infrared spectra of the two dimers are completely different. Isomer 2 absorbs almost at the same frequency as the monomer, with a small shoulder on its low frequency side. The similarity to the monomer spectrum implies that the CH bonds of the absorbing UV chromophore are most likely not directly affected by dimerization. That would be the case in a sandwiched or parallel-displaced geometry. Alternatively, it could be a T-shaped structure with only a weak CH···π interaction like the benzene dimer [7–10]. In that case the CH stretching vibrations are only shifted by 2–3 $cm^{-1}$ compared to the benzene monomer.

By contrast the infrared spectrum of isomer 1 (top trace in Fig. 2) shows five reproducible absorptions at 3022, 3046, 3052,

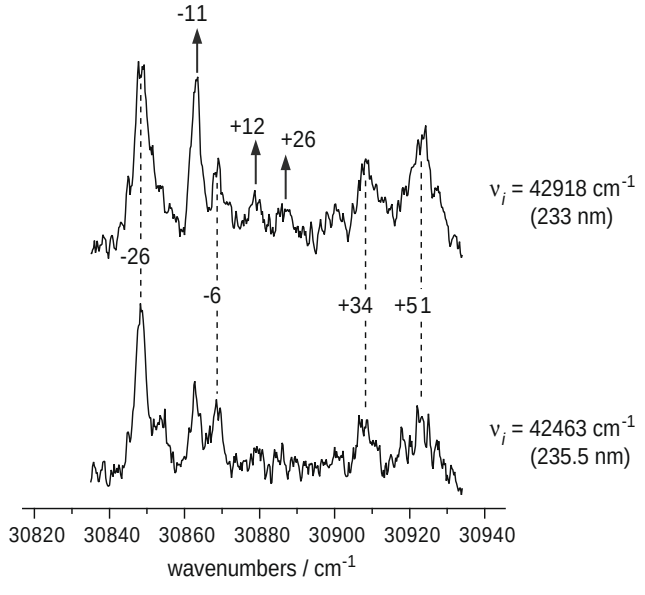


**Fig. 1.** Two-color R2PI spectra of pyrazine dimers ($Pz_2$) in the region of the $0_0^0$ band of pyrazine. The spectra were measured at different ionization laser energies of $\nu_i = 42,463$ $cm^{-1}$ (bottom) and 42,918 $cm^{-1}$ (top). At higher ionization energies several bands gain intensity (arrows), indicating the presence of a second isomer [16,15]. Frequency shifts are given relative to the monomer $0_0^0$ band at 30,876 $cm^{-1}$ [31].

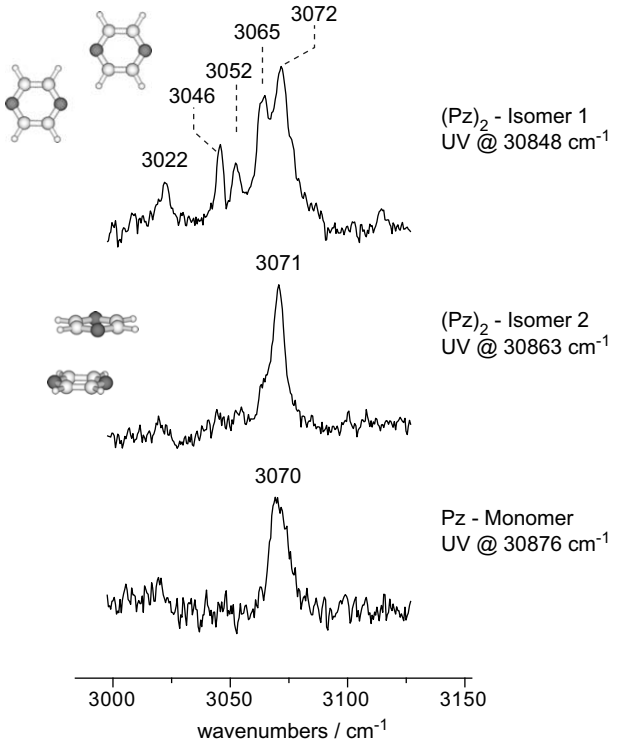


**Fig. 2.** IR–UV double resonance spectra of the two pyrazine dimer isomers ($Pz_2$, top two traces) and the pyrazine monomer (bottom). The molecules/clusters were excited at their respective $0_0^0$ origins and ionized at 233 nm (dimers) or 193 nm (monomer).

3065 and 3072 $cm^{-1}$. As mentioned earlier, no fragmentation of the dimer or of larger clusters has been detected. Therefore all observed bands belong to isomer 1. The number of bands and the observed frequency shifts, relative to the monomer absorption point to a direct involvement of the CH bonds of one or of both pyrazine molecules in CH···π or, more likely, CH···N interactions. We tend to rule out CH···π interactions because the effect on the CH stretching frequencies is rather small, as was demonstrated for the benzene dimer [33,12].

Our conclusions are confirmed by B3LYP-D and RI-MP2 calculations of several isomeric pyrazine dimers. Fig. 3 graphically illustrates the optimized structures of all stable isomers we have found, sorted with increasing B3LYP-D energy. The dimerization energies $E(dimer) - 2E(monomer)$ (including zero-point energy, ZPE) for both methods and for the TZVP and TZVPP basis sets are listed in Table 1. Dimerization energies provide a direct comparison between different methods and basis sets. The MP2 results in Table 1 and Fig. 4 are in agreement with the work of Mishra and Sathyamurthy [17], but they fixed the molecular geometry of the monomer units in the dimer calculations, which is not adequate for such weakly bound systems [18].

The cross-displaced, stacked dimer (isomer B in Fig. 3) is part of the so called S22 training set [34] and, consequently, has been the subject of several benchmark studies, including DFT-D calculations [35,36]. They all predict DFT-D stabilization energies in good agreement with the CCSD(T) benchmark value, while MP2 calculations yield a higher stabilization energy by up to 100% (see Table 1 and Ref. [17]). MP2 and MP4 calculations are known to overestimate the stability of the benzene dimer [37], whereas DFT-D calculations are again in good agreement with the CCSD(T) benzene dimer energies [35,36]. This is also illustrated in Fig. 4 where we

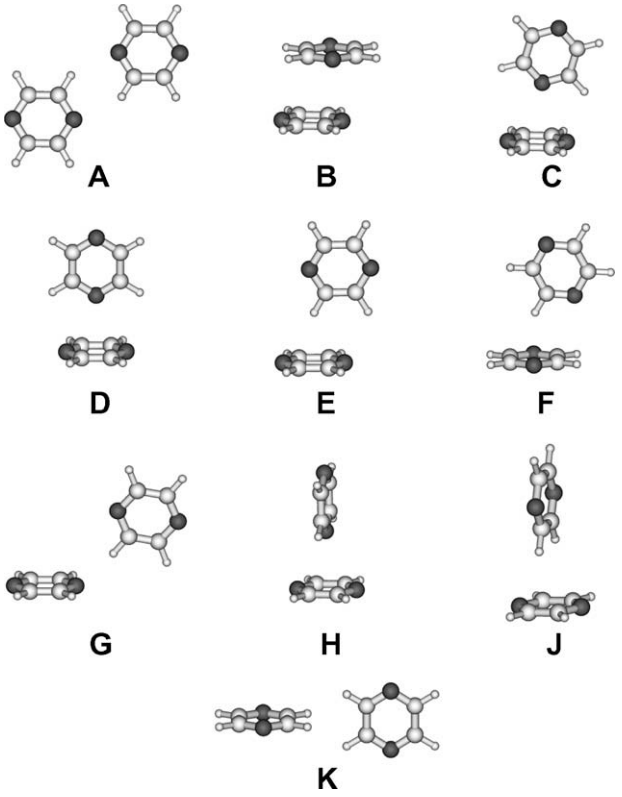


**Fig. 3.** Schematic representation of the calculated pyrazine dimer structures, sorted with increasing B3LYP-D/TZVP energy. The most stable dimer (A) has two stabilizing CH···N hydrogen bonds, while the second most stable dimer (B) is the well known stacked, cross-displaced dimer.

**Table 1**
Dimerization energies $[E(dimer) - 2E(monomer)]$ (including ZPE, in kJ $mol^{-1}$) of various pyrazine dimer structures at different levels of theory. See Fig. 3 for a graphical representation of the structures.

| Isomer | B3LYP-D | | RI-MP2 | |
|---|---|---|---|---|
| | TZVP | TZVPP | TZVP | TZVPP |
| A | −17.8 | −16.7 | −14.5 | −14.2 |
| B | −14.8 | −14.6 | −30.5 | −24.0 |
| C | −13.4 | −12.9 | –[a] | −15.8 |
| D | −12.8 | –[a] | −20.5 | –[a] |
| E | −10.3 | (−10.7)[b] | −12.7 | −10.4 |
| F | −9.7 | (−10.5)[b] | −14.3 | (−11.5)[b] |
| G | −9.5 | –[a] | −8.3 | −6.8 |
| H | −7.1 | −6.8 | −14.0 | −9.6 |
| J | (−6.6)[b] | (−6.7)[b] | −6.2 | (−7.1)[b] |
| K | −2.1 | −2.5 | 0.5 | −0.4 |

[a] Geometry optimization did not converge to a stable structure.
[b] Imaginary frequency. The values have only been included for comparison, by neglecting the imaginary frequency in the zero-point energy.

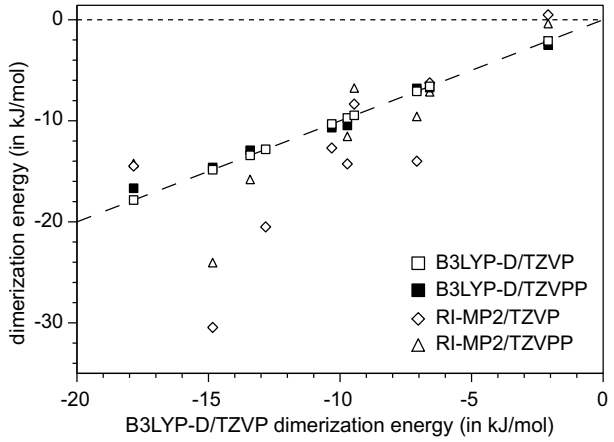


**Fig. 4.** Dimerization energies $[E(dimer) - 2E(monomer)]$ of various pyrazine dimer structures at different levels of theory plotted as a function of the B3LYP-D/TZVP dimerization energy. Both RI-MP2 and B3LYP-D yield similar stabilities for the CH···N hydrogen-bonded dimer, while MP2 overestimates the stability of the T-shaped and stacked isomers, where dispersion has a larger contribution to the overall stability. See Table 1 and Fig. 3 for a key to the respective dimer structures.

plotted the dimerization energies of Table 1 as a function of the B3LYP-D/TZVP energies. The latter has been chosen as reference, because it has the largest set of stable local minima of all our calculations. From Fig. 4 it is apparent that the predicted MP2 stabilities are much larger than the DFT-D values, but only for those isomers which have large contributions of dispersion interactions to the overall stability. On the other hand, both methods yield similar dimerization energies for the planar, doubly-bridged dimer A (Fig. 3). It is the most stable isomer in our B3LYP-D calculations and is stabilized by two CH··· N contacts. In this case the agreement between B3LYP-D and RI-MP2 calculations is expected, because both methods provide reasonable descriptions of clusters which are stabilized mainly by hydrogen bonding. Overall B3LYP-D seems to give a reliable description of the potential energy surface of the pyrazine dimer.

In order to facilitate an assignment of the experimental infrared spectra (Fig. 2) to individual cluster structures, we also calculated harmonic vibrational frequencies for each predicted isomer. The results of the B3LYP-D/TZVP calculations are shown in Fig. 5 as stick spectra. Also shown are the infrared spectra of isomers 1 and 2. Relative energies (in kJ $mol^{-1}$) are given in parenthesis.

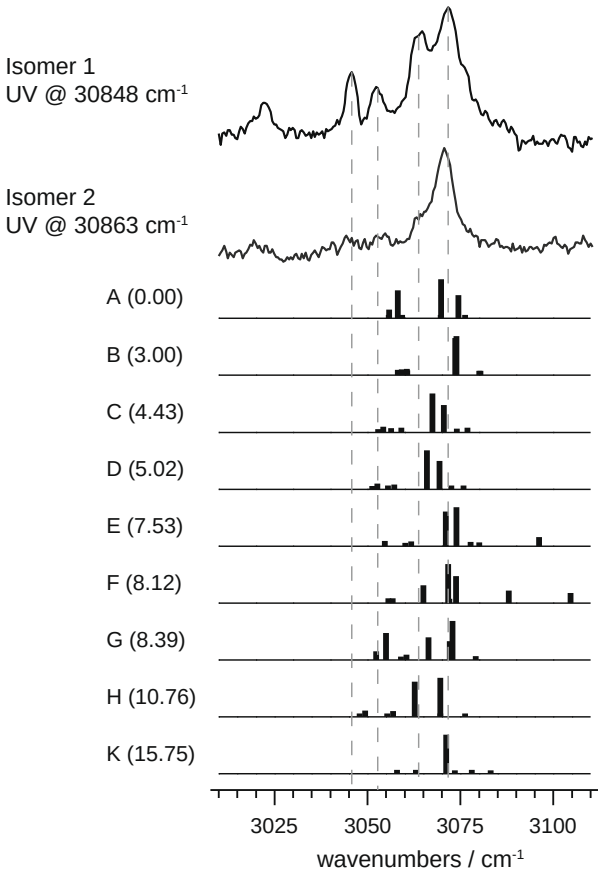


**Fig. 5.** Comparison of the experimentally obtained infrared spectra of isomers 1 and 2 with calculated and scaled stick spectra at the B3LYP-D/TZVP level. Calculated harmonic frequencies were scaled by 0.9694 in order to match the experimental and calculated CH stretching frequency of the pyrazine monomer. Relative dimer energies (in kJ $mol^{-1}$) at the B3LYP-D/TZVP level are given in parenthesis.

Almost identical spectra were obtained at the B3LYP-D/TZVPP level. MP2 calculations showed only minor differences.

Following our earlier argument, isomer 1 probably involves direct CH···N contacts. Among the structures in Fig. 3 such a direct interaction is only present in isomers A and G. Since dimer G is 8.39 kJ $mol^{-1}$ higher in energy, we assign the spectrum of isomer 1 to the planar, doubly-bridged most stable dimer A. Its stick spectrum is in qualitative agreement with the experiment, though the overlap is not perfect. The origin of the absorption at 3022 $cm^{-1}$ remains unclear. Pyrazine itself has a weak CH stretching absorption at 3018 $cm^{-1}$ [30] that is not discernible at the signal-to-noise level in Fig. 2 and might gain intensity in the dimer. Another possibility is Fermi resonance between the strong CH stretching vibrations and overtones or combination bands of ring stretching or of CH bending vibrations of the same symmetry. The energetic resonance condition of the Fermi coupling might be favored by the observed frequency shifts in the hydrogen-bonded dimer A and explains the absence of a corresponding band in the spectrum of the stacked isomer B [20]. The doubly-bridged, planar dimer structure is comparable to related aromatic NH···N hydrogen bonded dimers like the pyrazole dimer [19], where the planar structure dominates because of the larger strength of CH···N hydrogen bonds compared to CH···N interactions.

Isomer 2 shows only a single strong absorption in agreement with the calculated spectra of structures B and K. They are the only isomers which show a single strong IR absorption with all other vibrations having almost zero intensity. We assign the spectrum of isomer 2 to the stacked, cross-displaced structure B because of its higher stability. There the CH bonds are only indirectly influenced by the π-stacking and the vibrational frequencies of the individual pyrazine units are almost identical to those of the monomer. The absorption at 3071 $cm^{-1}$ of isomer 2 (Fig. 2) is then an overlap of the bands of the two symmetrically inequivalent pyrazine subunits. The T-shaped structures C and D are only 1.4 and 2.0 kJ $mol^{-1}$ higher in energy than B, but there the CH bonds of the stem are more directly influenced by dimer formation. As a consequence the vibrational frequencies of the top and stem molecules differ and the calculated spectra show two bands of similar intensity $\approx 4$ $cm^{-1}$ apart. Such a splitting is well within the resolution of our experiment but is not observed in the infrared spectrum of isomer 2.

Recently, the T-shaped structure of the benzene dimer has been verified by IR/UV double resonance experiments of isotopically mixed ( $C_6H_6$)($C_6D_6$) dimers by Meijer and co-workers [12]. They utilized the observation that only the stem benzene molecule of the T-shaped dimer has a sharp and intense UV absorbtion [7–10]. In combination with the isotopic shift of the UV absorption this allows for the selective detection of mixed dimers, depending on whether the stem is deuterated or not. Different IR spectra were obtained for the stem and top benzene molecule in agreement with a T-shaped structure [12]. Similar experiments for the pyrazine dimer have not been performed yet. For the stacked, cross-displaced pyrazine dimer most likely both monomer units have similar UV absorption intensities, so that a selective ionization of different pyrazine-$h_4$/pyrazine-$d_4$ is probably not possible, but high-level excited state calculations are needed to judge the nature of the UV excitations.

R2PI spectra of isotopically substituted and isotopically mixed pyrazine dimers have been published by Wanna and Bernstein [16]. They assigned isomer 1 to the T-shaped structure, while our IR/UV double resonance spectra identify isomer 1 as the planar hydrogen-bonded dimer. However, the authors argued that the red-most UV band belongs to the top and the other bands to the stem pyrazine molecule. If the UV bands could indeed be assigned to the respective monomer units, only then measurements of isotopically mixed dimers could allow for a selective ionization of different isotopomers and the infrared spectra could provide more detailed information about the cluster structure. Unfortunately, the signal-to-noise ratio of the vibronic bands at +12 and +26 $cm^{-1}$ of isomer 2 is too low for IR/UV double resonance experiments.

## 4. Summary

We presented the IR–UV double resonance spectrum of two pyrazine dimers in supersonic jets. Isomer 1 has a planar structure, stabilized by two CH···N contacts, while isomer 2 is the well known cross-displaced, stacked dimer. The assignment is supported by B3LYP-D/TZVP calculations. Until now we have no indication for the presence of a T-shaped structure. Isomers 1 and 2 are the two most stable structures in our B3LYP-D calculations, while MP2 probably tends to overestimate the stability of the stacked and T-shaped structures. Our results are in agreement with previous theoretical work on pyridine dimers [18]. It should be noted that the most stable doubly-bridged dimer, which is present in supersonic jets, does not directly reflect the structural motif of the pyrazine crystal [3–5]. The latter is formed by CH···N catemer synthons rather than dimers [3], although both are stabilized by CH···N contacts. Future experiments are planned to investigate pyrazine trimers and tetramers. These clusters could profit from a combination of stacking and CH...N interactions and could adopt a local configuration similar to the catemer synthons.

## Acknowledgement

This work has been supported by the Deutsche Forschungsgemeinschaft (FOR 618-TPE).

## References

[1] G.R. Desiraju, T. Steiner, The Weak Hydrogen Bond, Oxford University Press, New York, 1999.
[2] S. Scheiner, Hydrogen Bonding: A Theoretical Perspective, Oxford University Press, New York, 1997.
[3] V.R. Thalladi, A. Gehrke, R. Boese, New J. Chem. 24 (2000) 463.
[4] P.J. Wheatley, Acta Cryst. 10 (1957) 182.
[5] G. de With, S. Harkema, D. Feil, Acta Cryst. B 32 (1976) 3178.
[6] K.S. Law, M. Schauer, E.R. Bernstein, J. Chem. Phys. 81 (1984) 4871.
[7] K.O. Börnsen, H.L. Selzle, E.W. Schlag, J. Chem. Phys. 85 (1986) 1726.
[8] B.F. Henson, G.V. Hartland, V.A. Venturo, P.M. Felker, J. Chem. Phys. 97 (1992) 2189.
[9] W. Scherzer, O. Krätzschmar, H.L. Selzle, E.W. Schlag, Z. Naturforsch. A 47 (1992) 1248.
[10] V.A. Venturo, P.M. Felker, J. Chem. Phys. 99 (1993) 748.
[11] R. Schmied, P. Çarçabal, A.M. Dokter, V.P.A. Lonij, K.K. Lehmann, G. Scoles, J. Chem. Phys. 121 (2004) 2701.
[12] U. Erlekam, M. Frankowski, G. Meijer, G. von Helden, J. Chem. Phys. 124 (2006) 171101.
[13] U. Erlekam, M. Frankowski, G. von Helden, G. Meijer, Phys. Chem. Chem. Phys. 9 (2007) 3786.
[14] R.A. DiStasio Jr., G. von Helden, R.P. Steele, M. Head-Gordon, Chem. Phys. Lett. 437 (2007) 277.
[15] J. Wanna, J.A. Menapace, E.R. Bernstein, J. Chem. Phys. 85 (1986) 777.
[16] J. Wanna, E.R. Bernstein, J. Chem. Phys. 85 (1986) 3243.
[17] B.K. Mishra, N. Sathyamurthy, J. Theo. Comp. Chem. 5 (2006) 609.
[18] M. Piacenza, S. Grimme, Chem. Phys. Chem. 6 (2005) 1554.
[19] C.A. Rice, N. Borho, M.A. Suhm, Z. Phys. Chem. 219 (2005) 379.
[20] T.N. Wassermann, C.A. Rice, M.A. Suhm, D. Luckhaus, J. Chem. Phys. 127 (2007) 234309.
[21] T. Häber, K. Seefeld, K. Kleinermanns, J. Phys. Chem. A 111 (2007) 3038.
[22] I. Hünig, K. Kleinermanns, Phys. Chem. Chem. Phys. 6 (2004) 2650.
[23] C. Janzen, D. Spangenberg, W. Roth, K. Kleinermanns, J. Chem. Phys. 110 (1999) 9898.
[24] M. Gerhards, Opt. Commun. 241 (2004) 493.
[25] F. Weigend, M. Haeser, Theo. Chem. Acc. 97 (1997) 331.
[26] F. Weigend, M. Haeser, H. Patzelt, R. Ahlrichs, Chem. Phys. Lett. 294 (1998) 143.
[27] S. Grimme, J. Comput. Chem. 27 (2006) 1787.
[28] S. Grimme, J. Comput. Chem. 25 (2004) 1463.
[29] R. Ahlrichs, M. Bär, M. Häser, H. Horn, C. Kölmel, Chem. Phys. Lett. 162 (1989) 165.
[30] J.F. Arenas, J.T. Lopes-Navarrete, J.C. Otero, J.I. Marcos, J. Chem. Soc., Faraday Trans. 281 (1985) 405.
[31] J.E. Parkin, K.K. Innes, J. Mol. Spectrosc. 15 (1965) 407.
[32] K.B. Hewett, M. Shen, C.L. Brummel, L.A. Philips, J. Chem. Phys. 100 (1994) 4077.
[33] R.H. Page, Y.R. Shen, Y.T. Lee, J. Chem. Phys. 88 (1988) 4621.
[34] P. Jurečka, J. Šponer, J. Černý, P. Hobza, Phys. Chem. Chem. Phys. 8 (2006) 1985.
[35] C. Morgado, M.A. Vincent, I.H. Hillier, X. Shan, Phys. Chem. Chem. Phys. 9 (2007) 448.
[36] T. Schwabe, S. Grimme, Phys. Chem. Chem. Phys. 9 (2007) 3397.
[37] P. Hobza, H.L. Selzle, E.W. Schlag, J. Phys. Chem. 100 (1996) 18790.